Direct observation of charge-transfer-to-solvent (CTTS) reactions: Ultrafast dynamics of the photoexcited alkali metal anion sodide (Na^-)

Erik R. Barthel, Ignacio B. Martini, and Benjamin J. Schwartz[a)]
Department of Chemistry and Biochemistry, University of California, Los Angeles, Los Angeles, California 90095-1569

(Received 18 November 1999; accepted 6 March 2000)

Charge-transfer-to-solvent (CTTS) transitions have been the subject of a great deal of interest recently because they represent the simplest possible charge transfer reaction: The CTTS electron transfer from an atomic ion to a cavity in the surrounding solvent involves only electronic degrees of freedom. Most of the work in this area, both experimental and theoretical, has focused on aqueous halides. Experimentally, however, halides make a challenging choice for studying the CTTS phenomenon because the relevant spectroscopic transitions are deep in the UV and because the charge-transfer dynamics can be monitored only indirectly through the appearance of the solvated electron. In this paper, we show that these difficulties can be overcome by taking advantage of the CTTS transitions in solutions of alkali metal anions, in particular, the near-IR CTTS band of sodide (Na^-) in tetrahydrofuran (THF). Using femtosecond pump–probe techniques, we have been able to spectroscopically separate and identify transient absorption contributions not only from the solvated electron, but also from the bleaching dynamics of the Na^- ground state and from the absorption of the neutral sodium atom. Perhaps most importantly, we also have been able to directly observe the decay of the Na^-* excited CTTS state, providing the first direct measure of the electron transfer rate for any CTTS system. Taken together, the data at a variety of pump and probe wavelengths provide a direct test for several kinetic models of the CTTS process. The model which best fits the data assumes a delayed ejection of the electron from the CTTS excited state in ~700 fs. Once ejected, a fraction of the electrons, which remain localized in the vicinity of the neutral sodium parent atom, recombine on a ~1.5-ps time scale. The fraction of electrons that recombine depends sensitively on the choice of excitation wavelength, suggesting multiple pathways for charge transfer. The spectrum of the neutral sodium atom, which appears on the ~700-fs charge-transfer time scale, matches well with a species of stochiometry (Na^+, e^-) that has been identified in the radiation chemistry literature. All the results are compared to previous studies of both CTTS dynamics and alkali metal solutions, and the implications for charge transfer are discussed. © *2000 American Institute of Physics.* [S0021-9606(00)50221-9]

I. INTRODUCTION

Whenever a chemical species changes its electronic charge distribution during the course of a solution-phase chemical reaction, the surrounding environment undergoes a corresponding relaxation in response to this change. This solvent relaxation can in turn alter the electronic structure of the reacting species or induce nonadiabatic transitions, the result being that chemical reactivity in solution is controlled by the details of the solute-solvent coupling. This has prompted an explosion of experimental and theoretical interest in solvation dynamics, the study of the response of the solvent to the excitation of a probe solute.[1] The role of solvation dynamics and the solvent-induced nonadiabatic mixing of electronic states is especially important in controlling the dynamics of charge-transfer reactions, which are ubiquitous in chemistry and biology.[2]

The goal of better understanding solute-solvent coupling has led to a resurgence of interest in the study of what is perhaps the simplest charge-transfer reaction: electron transfer from a single atom to a cavity in the surrounding solvent.[3] The most prominent example of this type of electron transfer is that shown by halide ions in solution. Isolated halide ions in the gas phase support no bound electronic excited states, but in solution, these ions show an intense near-UV absorption at energies well below that required to create a free (vacuum) electron.[3] The nature of these solvent-supported states is not trivial, since the polar solvents that display this effect (water, nitriles, alcohols, etc.) do not possess low-lying orbitals that can accept an extra electron. Study of these spectra have had a rich history in chemical physics over the past 40 years, and they have become understood as charge-transfer-to-solvent (CTTS) transitions.[3,4] Photoexcitation of these transitions produces a neutral halogen atom and a solvated electron.[4] Gas phase studies[5] and *ab initio* quantum chemistry calculations[6] have concluded that CTTS transitions evolve from features present in gas phase clusters containing only a few solvent molecules: Localization of the continuum wave function of the ejected electron by the solvent molecules acts as a precursor to the states

a)Author to whom correspondence should be addressed; electronic mail: schwartz@chem.ucla.edu

comprising the CTTS band in the bulk liquid. It is the sensitivity of these purely electronic CTTS states to the solvent environment that makes them ideal candidates for investigating how local solvent structure, solvent-induced radiationless relaxation, and solvation dynamics work together to control electron transfer reactions.

The solvent dynamics underlying the CTTS transitions of aqueous halides recently have been explored in a series of quantum molecular dynamics simulations by Sheu and Rossky[7] and also by Staib and Borgis.[8] The simulations show that both the parent atom core and the polarized solvent molecules around the ion play a role in supporting the CTTS energy levels. The CTTS spectra are found to have a complex substructure consisting of a series of unresolved transitions from the *p*-like ground state orbital to states of mixed *s* and *d* character. Electron transfer from the excited CTTS states is driven by solvent fluctuations, with the symmetry of the one-electron state playing a critical role in the detachment dynamics: detachment takes place from only the lowest, predominantly *s*-like state. The simulations also predict that the solvated electrons produced following CTTS excitation remain in intimate contact with their parent atoms and thus can easily undergo geminate recombination.[7,8]

In a series of pioneering experiments, Long, Eisenthal, and co-workers[9] as well as Gauduel and co-workers[10] studied the dynamics of the electron detachment from aqueous halides using ultrafast pump–probe spectroscopy. The limitations of the femtosecond laser sources available at the time of these experiments, however, required the use of multiphoton excitation. Due to the symmetries of the various states involved, multiphoton excitation accesses states higher than the principal CTTS transition, leading to the possibility of competing channels for electron production. Thus, the hydrated electrons probed in these[9,10] and other experiments[11] are likely produced not only by electron transfer from the CTTS band, but also by direct photodetachment of the halide and possibly by multiphoton ionization of the solvent, obscuring the underlying CTTS dynamics.[7]

Bradforth and co-workers recently have revisited the transient spectroscopy of aqueous iodide, taking care to ensure that excitation was single-photon directly into the CTTS band.[12] These workers found that the dynamics of geminate recombination following CTTS were quite different from those produced following multiphoton ionization of the neat solvent, consistent with the idea that electron transfer via CTTS and direct photodetachment represent distinct mechanisms for electron production. The time scale for appearance of the electon, however, was observed to be similar for excitation of the CTTS transition and for multiphoton ionization of the pure solvent. Because the CTTS excited state could not be observed directly, Bradforth and co-workers could assign only an upper limit of $\sim$200 fs for the time scale of charge transfer.[12] Both the rapid CTTS dynamics in water and the observation of fast recombination are roughly consistent with the predictions of the quantum simulations discussed above; the experiments are only now becoming detailed enough to provide for a direct confrontation with theory.[13]

There are several reasons why aqueous halides prove to be difficult experimental systems for studying CTTS dynamics. First, the CTTS transitions are fairly deep in the UV ($\sim$230 nm for I^-), a region where even modern ultrafast lasers are hard-pressed to provide a conveniently tunable source of light. This makes pump wavelength-dependent experiments difficult, and also effectively prevents ground state bleach experiments which could access information on the equilibrium CTTS fluctuations. In addition, careful control over the intensity is critical with UV femtosecond pulses to avoid multiphoton ionization of the solvent. Second, the CTTS dynamics of halides in water or alcohols are extraordinarily fast, making it difficult experimentally to isolate the primary events leading to electron transfer. Finally, the reaction dynamics can be monitored only through the absorption of the solvated electron produced following charge transfer. It is unclear whether either the excited CTTS state[9] or the neutral halogen atom product is spectroscopically accessible; thus, the details of the intricate solvent dynamics that drive the electron transfer in these systems remain obscure.

In this paper, we demonstrate that all of these difficulties can be overcome by taking advantage of the CTTS transitions of alkali metal anions. The CTTS transition of sodide (Na^-) is conveniently located near 800 nm, the fundamental wavelength of the Ti:Sapphire laser, providing experimental accessibility to the ground state bleach dynamics as well as the possibility for experiments with tunable excitation. The excitation is one-photon directly into the CTTS band, and the use of visible/near-IR wavelengths ensures that there are no worries with multiphoton ionization of the solvent. Solutions of alkali metal anions can be prepared in a variety of solvents, providing the opportunity to study CTTS dynamics not only in systems with solvation dynamics as fast as those in water, but also in systems with dynamics that are significantly slower. Finally, as we will discuss below, the optical transitions of the neutral sodium atom produced following CTTS are readily accessible in the near-IR and are well separated from the absorption spectrum of the solvated electron in many solvents. This means that pump–probe experiments can independently monitor all three species involved in the CTTS reaction: the ground state Na^- bleach, the absorption of the neutral Na atom, and the absorption of the solvated electron are all readily observable. In addition, we also will show below that the excited CTTS state, Na^-*, can be probed directly in the visible region of the spectrum.

The selection of Na^- as the system of choice for the study of CTTS dynamics is predicated on a large number of studies of alkali metal anion solutions over the past 30 years.[14–17] Sodium anions are formed by the dissolution of the parent sodium metal in ether or amine solvents in the presence of a cation complexing agent.[14] The Na^+ complexing agent, usually a crown ether or cryptand molecule, drives the equilibrium $2Na_{(s)} \rightarrow Na^+ + Na^-$ far to the right, producing ample amounts of the solvated metal anion. (The actual equilibria describing the relationship between the solid alkali metal, metal anions and cations, and solvated electrons are a bit more complex; see Ref. 14 for details.) NMR experiments indicate that the sodium anion does not significantly complex with the solvent,[18] which, in combination with numerous optical studies[14,15] leads to the conclusion that the intense

visible/near-IR absorption band is indeed a CTTS transition. The absorption spectra of solvated electrons in the ethers and amines used to make alkali metal anion solutions are well known[19] and usually lie well to the red of the CTTS band. Less is known about the absorption spectrum of neutral sodium atoms in solution. Upon irradiation of solutions containing sodium cations, however, several studies have identified a species with stochiometry Na^0 [often referred to as a sodium cation:solvated electron contact pair (Na^+; e^-) in the literature], which has a broad absorption in the near-IR.[20] In this paper, we will argue that the neutral species produced immediately following CTTS has the same absorption spectrum as that in the pulsed radiolysis studies, leading to the identification of this species as a solvated neutral sodium atom.

The CTTS transition of sodide also offers an interesting contrast to the previous experimental and theoretical work on halides because of symmetry. As pointed out above, the outermost electron in the halides is in a *p*-like orbital; excitation of the CTTS band produces an excited state of predominantly *s* symmetry that can undergo detachment to form the *s*-like ground state of the solvated electron. For Na^-, however, the ground state CTTS electron is in an *s*-like orbital, so the Na^-* excited state is presumably *p*-like in character. In fact, we expect the electronic structure of the CTTS band in Na^- to be like that of the hydrated electron, consisting of three $s \rightarrow p$ transitions that are split by the local asymmetry of the solvent environment.[21] This hypothesis is supported by the strong similarity between the absorption spectrum of the hydrated electron and that of Na^-. The *p*-like symmetry of the excited sodide CTTS states suggests that the underlying charge-transfer mechanism may be quite distinct from that in the halides. One possibility is that large-scale solvent fluctuations may be required to induce a nonadiabatic transition from the *p*-like Na^-* state to produce the nodeless wave function of the solvated electron product. Another possibility is that the solvated electron may be produced directly in one of its excited states, and only later undergoes internal relaxation to the ground state.

In this paper, we present the results of a series of pump–probe experiments on the CTTS dynamics of Na^- in THF which are aimed at providing a preliminary exploration of all these possibilities. Like the previous work of Bradforth and co-workers,[12] we see the delayed appearance of solvated electrons following direct one-photon excitation of the CTTS band. We also find that the fraction of the electrons produced that undergo geminate recombination depends sensitively on the pump wavelength, suggesting multiple pathways for charge transfer. A transient absorption characteristic of the CTTS excited state is identified in visible probe experiments; the decay of this absorption in ~700 fs provides a direct measure of the charge transfer rate. Near-IR probe experiments monitor the appearance of the neutral sodium atom on the same ~700-fs time scale. In combination, the data provide enough information to build a kinetic model for the dynamics of all the species involved in the charge-transfer process.

II. EXPERIMENT

While alkali metal anions can be prepared from a variety of alkali metals in many different solvents, we believe that the Na^-/tetrahydrofuran (THF) system is the optimal choice for optical studies of CTTS dynamics. Preparation of solutions of alkalides other than Na^- (such as K^-) is complicated by contamination of small amounts of sodium leeched from the glassware.[22] This is because the equilibrium constant for the reaction $M^- + Na^+ \rightarrow Na^- + M^+$ (M=K, Rb, or Cs) lies far to the right, so the presence of even small amounts of sodium makes it difficult to prepare pure solutions of M^-.[14] Sodide solutions, on the other hand, are easy to prepare in high purity since, in the presence of excess sodium, any other alkali metals react away to produce more of the desired Na^-. Our choice of THF as the solvent is predicated on the fact that the dissolution of alkali metals in THF does not produce solvated electrons.[14] Thus, Na^-/THF solutions can be easily prepared with high purity, and with no solvated electrons present at equilibrium, it is straightforward to monitor the appearance of the electrons produced following excitation of the CTTS transition.

Sodide samples in tetrahydrofuran were prepared using an adaptation of the procedure of Dye and co-workers.[23] The samples were both synthesized and studied in a homemade container consisting of a 1-mm path length fused silica spectrophotometer cell which was joined to a Teflon stopcock with a graded glass seal. Sample synthesis was accomplished by loading the reagents into the cell in the inert atmosphere of a nitrogen dry-box. The stopcock was then closed before removal from the dry-box so that the sample could be studied on the optical table without ever contacting the ambient environment. Once sealed this way, the samples were typically stable for several weeks if stored in the dark at −20 °C. All of the synthesis and optical experiments reported in this paper, however, were performed at room temperature.

The three reagents needed to synthesize Na^-, Na metal, THF and 15-crown-5 ether (1,4,7,10,13-pentaoxocyclopentadecane), were obtained from Aldrich. Sodium metal and the crown ether were used as received; THF was dried over potassium metal before use. Sodium metal is not directly soluble in THF so a small amount (~10 mg) of potassium metal (whose cation has a higher affinity for the 15-crown-5 ether than the sodium cation) is used to catalyze the dissolution of ~100-mg sodium. Chunks of the two metals were placed in the cell and immersed in ~1 mL of a 1:200 v/v 15-crown5:THF solution. The sample was then agitated by sonication until a uniform dark blue color was obtained, indicating dissolution of the metals. The presence of sodide (λ_{max}=730 nm in THF) was confirmed by UV-visible absorption spectroscopy (see Fig. 1 below). The solutions produced at this point were usually too concentrated for spectroscopic measurements (optical density ~5 in the 1-mm cell at 730 nm). Thus, samples were further diluted with dry THF until the desired concentration (o.d.≤2 at 730 nm) was reached.

While preparation of the sodide samples following the procedure of Dye *et al.* was straightforward,[23] we had to try several synthetic variations to produce samples that were stable for more than a few hours and were not easily

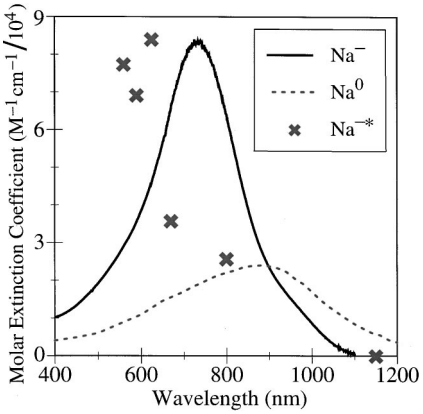

FIG. 1. Absorption spectra of the species involved in the CTTS reaction of sodide. The solid curve shows the absorption spectrum of the Na^-/THF samples used in this study; the absolute value of the molar extinction coefficient for this curve at the 730-nm absorption maximum was scaled to match that in Ref. 17. The dashed curve shows the absorption spectrum of the Na^0 species in THF with data provided by John Miller (see also Ref. 20). The crosses show the absorption spectrum of the Na^{-*} excited state as determined by fitting the data in Figs. 3 and 4 to the ''delayed ejection'' model [Eq. (9), Table I]; see text for details.

bleached by exposure to the femtosecond laser pulses. The key to producing stable samples is to place enough sodium metal in the cell to maintain an excess of metal after dissolution. The underlying idea is to saturate the solution with metal at a given crown ether concentration. This way, as sodium anions are destroyed by impurities or by dissociation with the laser, additional anions can be generated by dissolution of the excess metal. The overall concentration of sodide is thus controlled by the fixed amount of crown ether, allowing the samples to be diluted and to remain stable for several weeks.

The presence of potassium metal in the samples means that there is a possibility that potasside can form after the samples age and the excess Na metal is depleted. The absorption spectrum of our sample can be fit to a superposition of the known absorption spectra of Na^- ($\lambda_{max}=730$ nm) and K^- ($\lambda_{max}=950$ nm).[14,17] The results suggest that the relative concentration of potasside in freshly prepared samples is less than a few percent. The height of the 950-nm shoulder due to K^- grows slowly with time as the excess sodium is depleted; the fits indicate that the relative concentration of K^- can reach $\sim 25\%$ in samples that are several months old. At this point, it is unclear whether production of K^- is accelerated by exposure to the femtosecond laser pulses or merely correlates with sample longevity. In any case, for the experiments reported below we have chosen excitation wavelengths (near 500 nm) on the blue side of the Na^- CTTS absorption where K^- does not absorb, thus avoiding adverse effects from a possible build-up of K^- during the course of the femtosecond experiments.

The laser system used in the time-resolved experiments consists of a regeneratively amplified Ti:sapphire laser (Spectra Physics) that produces 1-mJ, $\sim$120-fs pulses centered at 800 nm at a 1 kHz repetition rate. The output is used to pump a dual-pass optical parametric amplifier (OPA) that generates tunable signal and idler beams in the IR. For most experiments, either the signal or idler beam (or both) are subsequently sum frequency mixed with the residual 800-nm light in a BBO crystal to produce tunable pump and/or probe laser pulses throughout the visible region of the spectrum.[24] Other experiments used either the 800-nm fundamental or the signal or idler beams (or harmonics thereof) directly as the probe pulse. For all experiments, the probe beam is split into reference and signal components; the pump and probe signal beams are focussed collinearly to a ~ 300-μm spot at the sample. The relative polarizations of the pump and probe beams are set to the magic angle (54.7°). The signal and reference pulses are detected either by matched Si photodiodes (probe wavelengths <1100 nm), or by matched InGaAs photodiodes (probe wavelengths $\geqslant 1100$ nm). The output from the photodiodes is digitized on a shot-to-shot basis by a fast gated current-integrating analog-to-digital converter. Pulse intensities outside preset bounds are rejected from the data collection on the fly; the remaining pulses are normalized (signal/reference) on every shot. The pump beam is also chopped and in-house software is used to digitally lock the baseline while scanning the mechanical pump–probe delay;[25] typical noise levels for averaging 300 laser shots per stage position are changes in optical density of $\sim 2\times 10^{-4}$. The instrument function and position of time zero is found for each combination of wavelengths by measuring the pump-probe cross-correlation using sum-frequency mixing in a BBO crystal placed at the position of the sample. Further details on the setup and data collection routines have been published elsewhere.[26]

The ultrafast spectral transients presented below were recorded with pump pulse energies of ~ 1 μJ, resulting in changes in optical density on the order of a few tenths of a percent. After the initial dynamics in the first few ps are complete, all the spectral transients presented below persist for times much longer than the length of the translation stage used to generate the pump–probe delay ($\geqslant 1$ ns). The long time behavior of the transients was measured by flash photolysis using $\sim$10-ns pulses at 532 nm from a doubled Nd:YAG laser to excite the samples and an arc lamp to probe. The bleach signals were found to persist out to times of a few ms. The long recovery time could be explained either by diffusive, nongeminate recombination of the CTTS products to reform the parent Na^-, or by diffusion of additional ground state Na^- ions into the volume sampled by the probe beam. The long time scale for sample recovery means that in the femtosecond experiments, there is the possibility that the photoproducts produced by one laser pulse are still present when the next pulse arrives at the 1-kHz repetition rate. To ensure that build-up of the photolysis products did not obscure the underlying CTTS dynamics, we performed the pump–probe experiments while the repetition rate of the laser was varied from 50 Hz to 1 kHz. At all repetition rates, the transient dynamics were identical, indicating that none of the long-lived species produced following excitation adversely affected our study of the short-time CTTS dynamics.[27] We also found that at high excitation fluences, the amplitude of the fast absorption decay in the transients decreased markedly, which as discussed below, is consistent

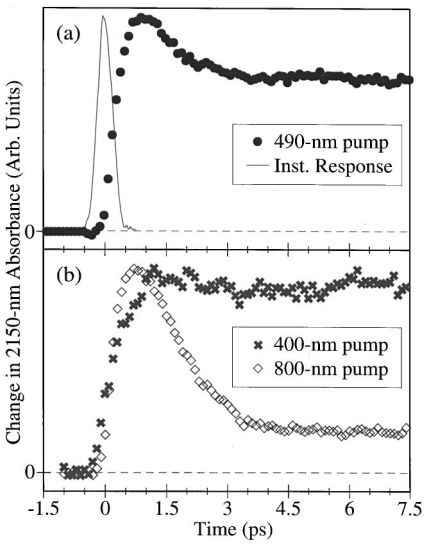

FIG. 2. (a) Appearance of the solvated electron's absorption at 2150 nm following femtosecond excitation of Na^-/THF at 490 nm (circles). The thin solid curve shows the experimentally measured instrument response. (b) Appearance of the solvated electron's absorption following femtosecond excitation of Na^-/THF at 400 nm (crosses) and 800 nm (diamonds). For both (a) and (b), the rise of the 2150-nm absorption is slower than the instrument response, indicating a delayed appearance of the electron.

with decreased geminate recombination due to multiphoton excitation of Na^-.

III. RESULTS

The solid curve in Fig. 1 shows the steady-state absorption spectra for the sodide anion in THF. The spectrum is in excellent agreement with those previously published;[14,15,17] because we are not able to independently measure the concentration of Na^- in our solutions, the *y*-axis showing the value of the molar extinction coefficient was scaled to match that in Ref. 17. As discussed in many studies, the intense absorption feature that peaks at 730 nm corresponds to a CTTS transition.[14,15] No previous flash photolysis studies,[16,17] however, have been able to measure the rate of production of solvated electrons following excitation of the Na^- CTTS transition. In THF, pulsed radiolysis studies have shown that the solvated electron absorption band occurs in the mid-IR, with a peak near 0.6 eV ($\sim$2100 nm) and a full width at half maximum of $\sim$0.3 eV.[19] Thus, final confirmation of the assignment of the optical absorption of Na^- to a CTTS transition awaits observation of the delayed appearance of the solvated electron band in the mid-IR correlated with excitation of the CTTS band.

Figure 2(a) provides this confirmation by presenting the results of femtosecond transient absorption experiments exciting on the blue side of the CTTS band at 490 nm and probing the solvated electron's appearance near the maximum of its absorption at 2150 nm (circles). The thin solid curve shows the cross-correlation between the pump and probe beams as measured by sum-frequency mixing in a BBO crystal placed at the position of the sample, and verifies that our instrument resolution is $\sim$250 fs. The data are qualitatively similar to that reported by Bradforth and co-workers on the iodide system[12] in that absorption by the solvated electron does not appear for a few hundred femtoseconds after excitation, presumably related to the time for electron transfer to take place from the excited CTTS state. After creation, the electron's 2150-nm absorption undergoes a decay which takes place on a $\sim$1.5-ps time scale. After the decay is complete, an absorption offset from the solvated electron persists for times much greater than a few nanoseconds. There are several possibilities for the assignment of the decay of the solvated electron's absorption. The electron's absorption cross-section could change with time due to dynamic solvation or to the presence of a nonadiabatic transition (from a *p*-like to *s*-like state, for example). On the other hand, the absorption decrease could represent a loss of population due to geminate recombination of a fraction of the CTTS-produced electrons with the nearby parent sodium atom.

To gain more insight into the origin of the observed absorption decay, the 2150-nm dynamics of the electron were monitored after excitation at different wavelengths, as shown in Fig. 2(b). The results show that there is a continuous increase in the magnitude of the decay as the excitation wavelength is tuned toward the red. Excitation at 400 nm (crosses) produces essentially no decay of the 2150-nm absorption; the 490-nm excitation scan presented in Fig. 2(a) shows an intermediate amplitude of the decay, while 800-nm excitation (diamonds) results in a nearly complete decay of the entire signal. It is unlikely that changes in the electron's absorption cross-section due to solvation dynamics or to transitions between quantized electronic states would be so strongly affected by the excitation wavelength. Instead, in direct analogy to numerous studies where solvated electrons are produced by multiphoton excitation,[28] the excitation wavelength dependence can be explained by differences in the population of the ejected electrons. An increase in the excitation energy allows a larger fraction of the ejected electrons to thermalize at distances further from the parent atom core, reducing the probability for geminate recombination and leading to less decay of the absorption signal.[28] The slightly longer rise time observed for 400-nm excitation is also consistent with a delayed appearance of the electron's equilibrium absorption due to the time needed to dissipate excess thermal energy.[29] We will return to the question of the wavelength dependence of geminate recombination later in this paper. Overall, Fig. 2 leads us to expect that geminate recombination of the neutral Na atom and solvated electron produced following CTTS excitation are an important part of the photophysics of Na^-.

Additional information concerning the mechanism of electron production and the nature of the CTTS band in sodide solutions is available from the transient absorption dynamics at various probe wavelengths in the visible and near-IR. From top to bottom, Fig. 3 shows the spectral dynamics of Na^- probed at 560 nm, 590 nm, 625 nm, 670 nm and 800 nm following excitation near 500 nm. All five of these probe wavelengths lie within the envelope of the Na^- ground state absorption (cf. Fig. 1), leading to the expectation of a transient bleach signal (an instantaneous negative change in absorbance) due to the loss of ground state Na^- following ex-

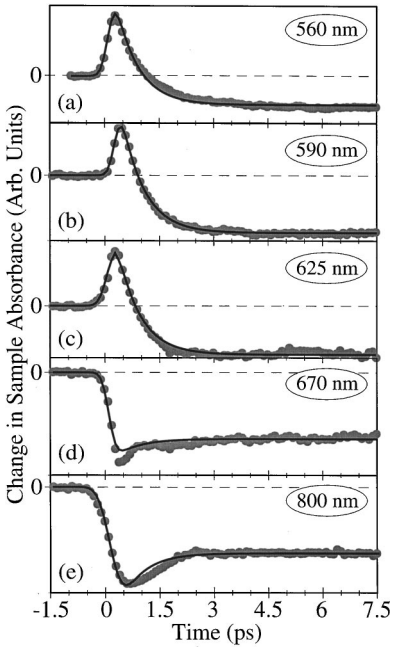

FIG. 3. Femtosecond absorption transients resulting from ~500-nm excitation of Na^-/THF and probing at (a) 560 nm, (b) 590 nm, (c) 625 nm, (d) 670 nm, (e) 800 nm. Negative signals correspond to bleaching of the Na^- ground state absorption; positive signals reflect absorption of excited-state species. The solid curves through the data points are nonlinear least squares fits to the ''delayed ejection'' model [Eq. (9); Table I]; see text for details.

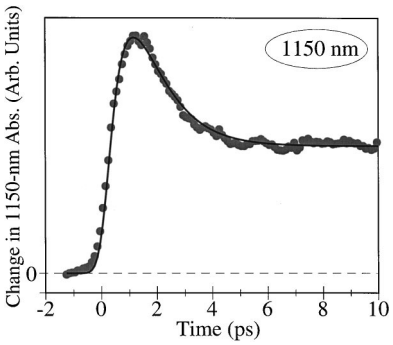

FIG. 4. Femtosecond transient absorption at 1150 nm resulting from 615-nm excitation of Na^-/THF. The solid curve through the data points is a nonlinear least squares fit to the ''delayed ejection'' model [Eq. (9), Table I]; see text for details.

citation. The two reddest probe wavelengths considered in Fig. 3, 670 nm and 800 nm, are near the maximum of the ground state CTTS band and indeed, the transient signals are bleaches that appear within the instrument resolution. These two bleach signals show decay dynamics with similar amplitude and time scale to that of the solvated electron [cf. Fig. 2(a)], suggestive of the reappearance of ground state Na^- ions due to recombination of the solvated electron and neutral sodium atom products. Finally, the bleach persists well past the ~1-ns limit of our scan range indicating that photoexcitation produces a net loss of ground state Na^- ions.

At the three bluest probe wavelengths shown in Fig. 3, on the other hand, the spectral transients are dominated by a strong absorption that appears within the instrument resolution and then rapidly decays in ~700 fs into a net bleach signal. The data indicate that the spectrum of this initial absorption must peak near 590 nm. The excited absorption band clearly spans the wavelengths between 560 and 625 nm, but there is no initial absorption at 670 nm or 800 nm. There also is no sign of an absorption (or corresponding rise of the bleach) when probing at 510 nm (not shown), a wavelength where any excited-state absorption would be readily apparent because of the small absorption cross-section of the ground state. Thus, we have identified the presence of a rapidly decaying excited-state species that absorbs predominantly in the spectral region centered near 590 nm.

The assignment of this 590-nm absorbing species is not immediately clear. The solvated electron product does not have significant absorption in this spectral region,[19] but there are still two other possibilities for absorbing species produced following excitation of Na^-. One candidate is the instantaneously formed Na^-* CTTS state. For this case, the rapid absorption decay would result from the loss of the initially prepared excited state due to the charge transfer process, and the absorption dynamics would provide a convenient spectroscopic handle for measuring the rate of electron transfer. The other possible assignment is that the absorbing species is the neutral sodium atom (Na^0) product,[30] which could be produced on a time scale faster than our instrumental resolution if CTTS were quite rapid. One might expect that immediately after removal of the excess electron, the solvent would not have a significant interaction with the neutral atom product, possibly leading to a strong Na^0 absorption near 590 nm similar to that of Na in the gas phase (the famous ''D'' line). Dynamic solvation would then cause the Na atom's spectrum to shift, providing an explanation for the rapid decay of the absorption in this spectral region.

How can we distinguish between these two possible interpretations of the data? On the basis of pulsed radiolysis studies, we expect the equilibrated Na^0 product in THF to have a broad absorption in the near-IR peaking near 890 nm (Fig. 1, dashed curve, adapted from Ref. 20). At 1150 nm, the ground state absorption of Na^- is negligible but the Na^0 species whose absorption spectrum is presented in Fig. 1 still has appreciable cross-section ($\sim 6000\ M^{-1}\ cm^{-1}$).[20] Thus, a femtosecond experiment probing at 1150 nm should provide a clean signature of the appearance of the equilibrated neutral sodium atom without interference from the bleaching dynamics of Na^-.[31] This information can help to distinguish between the two possible interpretations of the visible-probe data presented in Fig. 3. The results of such an experiment are shown in Fig. 4. Indeed, a species that absorbs at 1150 nm does appear with a rise time of ~700 fs. The 1150-nm transient absorption then undergoes a decay on the same time scale as the solvated electron at 2150 nm, followed by an offset that indicates the absorbing species persists for long times. The solvated electron in THF has only a small absorption cross-section at 1150 nm[19,31] and the excited CTTS state is expected to be short lived, so the majority of the persistent 1150-nm absorption must be due to the neutral sodium atom produced following CTTS.

The assignment of the 1150-nm absorption to the equilibrated Na^0 species, in combination with the data in Figs. 3

and 4, provides enough information to test two different models of the entire charge-transfer-to-solvent process. The first kinetic model we consider, the ''delayed ejection'' model, assumes that it takes some time for solvent fluctuations to cause the electron to detach from the initially prepared Na^-* state:

$$Na^- \xrightarrow{h\nu} Na^-*, \tag{1}$$

$$Na^-* \underset{k_1}{\xrightarrow{\text{CTTS}}} Na^0 \bullet e^-_{\text{solvated}}, \tag{2}$$

$$Na^0 \bullet e^-_{\text{solvated}} \underset{k_2}{\xrightarrow{\text{recombination}}} Na^-, \tag{3}$$

$$Na^0 \bullet e^-_{\text{solvated}} \underset{k_3}{\xrightarrow{\text{escape}}} Na^0 + e^-_{\text{solvated}}. \tag{4}$$

In this model, Eq. (1) indicates that photoexcitation instantaneously creates the CTTS excited state, presumably the source of the strong 590-nm transient absorption. The excited CTTS state then disappears with rate k_1, leading to a delayed appearance of the 1150-nm equilibrated Na^0 and 2150-nm solvated electron absorptions, as described by Eq. (2). Although we label the product in Eq. (2) as $Na^0 \bullet e^-_{\text{solvated}}$, we do not intend to imply that this is a species that is spectroscopically distinct from individual sodium atoms and solvated electrons. The idea of a ''contact pair,'' however, and in fact the entire model represented by Eqs. (1)–(4), is consistent with the simulations performed by Staib and Borgis.[8] Introduction of the contact pair into the kinetic model provides the mathematical convenience of being able to describe the subsequent geminate recombination using simple first-order kinetics with rate k_2 [Eq. (3)].[32] The model is completed by assuming that the contact pair can dissociate with rate k_3 [Eq. (4)], so that a fraction $f = k_2/(k_2+k_3)$ of the Na^0 and solvated electron species undergo recombination to regenerate some of the initially bleached parent Na^-. This recombination accounts for the fractional loss of the 1150-nm Na^0 absorption in Fig. 4, the 2150-nm solvated electron absorption in Fig. 2, and the visible Na^- bleach signals in Fig. 3. Note that for this model, we implicitly assume that solvation dynamics do not significantly affect the spectroscopy of either the Na^- ground state bleach or the absorption of the newly formed $Na^0 \bullet e^-_{\text{solvated}}$, solvated electron, or Na^0 products.

The measured signals $S(t)$ in the ''delayed ejection'' model consist of the sum of increases in absorption due to the formation of Na^-* and Na^0 (or $Na^0 \bullet e^-_{\text{solvated}}$) as well as the bleach of the Na^- ground state:

$$S(t) = \epsilon_{Na^-*}[Na^-*](t) + \epsilon_{Na^0}\{[Na^0 \bullet e^-_{\text{solvated}}](t) + [Na^0](t)\} + \epsilon_{Na^-}[Na^-](t), \tag{5}$$

where $[X](t)$ and ϵ_X are the time-dependent concentration change and the molar extinction coefficient, respectively, of each species ''X'' involved in the CTTS reaction. Note that in this notation, $[Na^-](t)$ will be negative, indicating a net loss of ground state population that corresponds to a transient bleach signal. The absorption of the solvated electron is neglected in Eq. (5) since it has a very small cross-section at the visible and near-IR probe wavelengths used in Figs. 3 and 4 ($\epsilon_{e^-} \ll \epsilon_{Na^-}, \epsilon_{Na^0}$).[31] The chemical reactions in Eqs. (1)–(4) lead to the following kinetic model for the concentrations of the various species involved in the CTTS reaction:

$$\begin{aligned}
\frac{d}{dt}[Na^-*](t) &= -k_1[Na^-*](t),\\
\frac{d}{dt}[Na^0 \bullet e^-_{\text{solvated}}](t) &= k_1[Na^-*](t) - (k_2+k_3)[Na^0 \bullet e^-_{\text{solvated}}](t),\\
\frac{d}{dt}[Na^-](t) &= k_2[Na^0 \bullet e^-_{\text{solvated}}](t),\\
\frac{d}{dt}[Na^0](t) &= \frac{d}{dt}[e^-_{\text{solvated}}](t) = k_3[Na^0 \bullet e^-_{\text{solvated}}](t),
\end{aligned} \tag{6}$$

subject to the boundary conditions:

$$\begin{aligned}
&[Na^-*](0) = -[Na^-](0) = N_0,\\
&[Na^0](0) = [Na^0 \bullet e^-_{\text{solvated}}](0) = 0,
\end{aligned} \tag{7}$$

where N_0 is the initial concentration of excited Na^-. After solving the coupled differential Eqs. (6) with the boundary conditions of Eqs. (7), the time dependent concentrations obtained are inserted into Eq. (5) to give the functional form of the signals measured in the pump–probe experiments:

$$\begin{aligned}
\frac{S(t)}{N_0} = {} & \epsilon_{Na^-*}\exp(-k_1 t) + \epsilon_{Na^0}\kappa k_1[\exp(-(k_2+k_3)t) - \exp(-k_1 t)] + \epsilon_{Na^0}\kappa k_3 \exp(k_1 t)\\
& - \epsilon_{Na^0}\kappa k_1 k_3 \chi \exp(-(k_2+k_3)t) + \epsilon_{Na^0} k_3 \chi\\
& + \epsilon_{Na^-}\kappa k_2 \exp(-k_1 t) + \epsilon_{Na^-}(k_2\chi - 1)\\
& - \epsilon_{Na^-}\kappa k_1 k_2 \chi \exp(-(k_2+k_3)t),
\end{aligned} \tag{8}$$

where $\kappa = (k_1 - k_2 - k_3)^{-1}$ and $\chi = (k_2+k_3)^{-1}$. Since the rate k_3 does not correspond to a process that can be directly measured spectroscopically, it makes more sense to recast the model in terms of the CTTS rate k_1, the recombination rate k_2, and the quantum yield for recombination f. From the definition of $f = k_2/(k_2+k_3)$, we can make use of $\chi = f/k_2$ and rewrite $\kappa = f/(fk_1 - k_2)$ to obtain:

$$\begin{aligned}
\frac{S(t)}{N_0} = {} & \epsilon_{Na^-*}\exp(-k_1 t)\\
& + \kappa \exp(-k_1 t)\left\{\epsilon_{Na^0}\left[k_2\left(\frac{1}{f}-1\right) - k_1\right] + k_2\epsilon_{Na^-}\right\}\\
& + \kappa k_1 f \exp(-(k_2/f)t)[\epsilon_{Na^0} - \epsilon_{Na^-}]\\
& + \epsilon_{Na^0}(1-f) + \epsilon_{Na^-}(f-1).
\end{aligned} \tag{9}$$

For the model represented by Eq. (9), the cross-sections of the Na^- ground state and Na^0 products at each wavelength are already determined (Fig. 1). Thus, not counting the overall amplitude scaling factor N_0 for each transient, there are only nine adjustable parameters for the six transients in Figs.

TABLE I. Fit parameters and probe wavelength cross-sections for the ''delayed ejection'' model [Eq. (9)].

Pump/Probe Wavelengths (nm)	(a) ϵ_{Na^-} ($M^{-1}\,cm^{-1}$)	(b) ϵ_{Na^0} ($M^{-1}\,cm^{-1}$)	(c) ϵ_{Na^-*} ($M^{-1}\,cm^{-1}$)	(c) k_1 (ps^{-1})	(c) k_2 (ps^{-1})	(c) f
505/560	29 970	9100	77 000	1.42±0.2	0.66±0.1	0.4±0.1
490/590	35 230	10 100	69 000	1.42±0.2	0.66±0.1	0.4±0.1
490/625	46 180	12 000	84 000	1.42±0.2	0.66±0.1	0.4±0.1
500/670	67 380	14 800	35 000	1.42±0.2	0.66±0.1	0.4±0.1
490/800	63 950	23 750	27 000	1.42±0.2	0.66±0.1	0.4±0.1
615/1150	~0	5800	0	1.42±0.2	0.66±0.1	0.7±0.1

[a]Parameters taken from absorption spectrum presented in Fig. 1 with maximum scaled to have the same cross-section as Ref. 17.
[b]Parameters supplied by John Miller (see also Ref. 20).
[c]Parameters found from the nonlinear least squares fit of the data in Figs. 3 and 4 to Eq. (9); k_1 and k_2 are constrained to be the same for all six pump–probe transients; f is constrained to have the same value for a given pump wavelength. The fitted Na^-* cross-sections have an uncertainty of ±15%.

3 and 4: The cross-section of the Na^-* excited state at each probe wavelength (which turns out to be zero for one of the six wavelengths), the CTTS and recombination rate constants k_1 and k_2, and the recombination fraction f. For comparison, a simple fit of each of these transients to a biexponential process (which cannot adequately describe all the data because of the long-time offsets on each scan) would involve 18 adjustable parameters (2 decay times and an amplitude ratio per transient) not counting the overall scaling amplitude.

The solid curves in Figs. 3 and 4 show a global nonlinear least squares fit of Eq. (9), convoluted with the experimentally measured instrument response at each wavelength, to all six of the various Na^- pump–probe transients. Given that on average there are only 1.5 adjustable parameters per transient, the fits do an excellent job describing the data. The best fit cross-sections for the Na^-* excited state at each wavelength are shown as the crosses in Fig. 1. The best fit times for the CTTS electron transfer and geminate recombination processes are $\tau_1 = 1/k_1 = 0.70 \pm 0.09$ ps and $\tau_2 = 1/k_2 = 1.5 \pm 0.2$ ps, respectively. The best fit fraction of recombination, f, for the visible transients in Fig. 3 is 0.4 ± 0.1. The fraction f used to fit the 1150-nm transient in Fig. 4 is a fair bit larger at 0.7 ± 0.1; the difference results from the redder excitation wavelength used for this experiment, which as discussed above leads to a higher fraction of recombination. All the fit parameters for this model are summarized in Table I.

The second kinetic model we consider to describe the data in Figs. 3 and 4 is the ''solvation model,'' which involves rapid charge transfer followed by dynamic solvation of the Na^0 product:

$$Na^- \xrightarrow[k_1]{h\nu,\mathrm{CTTS}} Na^0_{\text{``hot''}} + e^-_{\text{solvated}}, \tag{10}$$

$$Na^0_{\text{``hot''}} \xrightarrow[k_2]{\text{solvation}} Na^0_{\text{eqb}}, \tag{11}$$

$$f\,Na^0 + f\,e^-_{\text{solvated}} \xrightarrow[k_3]{\text{recombination}} f\,Na^-. \tag{12}$$

In this model, photoexcitation detaches the CTTS electron from Na^- to produce a ''hot'' (unsolvated) Na^0 atom and a solvated electron, as represented by Eq. (10). Since the excited absorption near 590 nm, which we would expect to come from ''hot'' gas-phaselike Na^0, appears instantaneously we would expect the rate k_1 to be faster than our ~250-fs time resolution. Once formed, the solvent relaxes around the ''hot'' Na^0, producing the equilibrated Na^0 species, which absorbs at 1150 nm, on the solvation time scale $1/k_2$ as described by Eq. (11). Then, like the ''delayed ejection'' model, some fraction f of the Na^0 species, either during solvation or after equilibration, undergo recombination with the solvated electron to regenerate the parent Na^- as shown in Eq. (12). This would lead to a fractional loss of the 1150-nm Na^0 absorption (Fig. 4), the 2150-nm solvated electron absorption (Fig. 2), and the visible Na^- bleach signals (Fig. 3), all with rate k_3.

According to the solvation model, the key spectral changes following excitation rely on the solvation dynamics that continuously shifts the absorption of Na^0 from near 590 nm to the equilibrated spectrum near 890 nm shown in Fig. 1 [Eq. (11)]. The dynamics of solvation in THF, however, already have been measured by Maroncelli and co-workers, who found that after excitation the emission spectrum of a dye molecule undergoes a biexponential Stokes shift with time scales 0.2 ps (45%) and 1.5 ps (55%).[33] We use this information as a constraint in the solvation model for CTTS excitation of Na^-: Once ''hot'' Na^0 is formed upon excitation, the rate at which the spectrum shifts with time is completely determined. Using the parameters for THF solvation from Maroncelli and co-workers, along with the fact that the oscillator strength of the Na^0 absorption must be conserved during the Stokes shift, we have solved numerically the appropriate kinetic equations and attempted to reproduce the signals measured in Figs. 3 and 4. The adjustable parameters are the absorption cross-sections for the ''hot'' Na^0 species at each probe wavelength, the fraction f of species that recombine, and the recombination rate k_3. The rate k_1 is assumed instantaneous, and ''k_2'' is the bi-exponential solvation process measured by Maroncelli and co-workers.

Upon fitting the data in Figs. 3 and 4 (not shown), it is apparent that the solvation model cannot adequately describe the observed pump–probe transients. The solvation model

fits the 560-nm, 590-nm, and 625-nm transients in Fig. 3 nearly as well as the delayed ejection model, but the solvation model predicts the wrong general shape to properly describe the two transients at 670 nm and 800 nm. The problem is that as the absorption maximum of Na^0 shifts from near 590 nm to its final position near 890 nm, the peak has to pass through both 670 nm and 800 nm. Thus, for these wavelengths, the model predicts a bleach signal which at first decays as the maximum of the Na^0 absorption arrives, but then rises again as the maximum of the Na^0 absorption shifts further to the red. We tried several variations of the model using different solvation parameters,[34] but all predict highly nonmonotonic bleach signals at 670 nm and 800 nm. In addition, the rise of the 1150-nm Na^0 absorption is not well described by the model since neither of the bi-exponential THF solvation times match the observed ~700-fs single exponential rise. Thus, we conclude that the solvation model represented by Eqs. (10)–(12) does not provide an adequate description of the data in Figs. 3 and 4.

IV. DISCUSSION

The success of the delayed ejection model in fitting the pump–probe transients allows the various features of the data to be readily interpreted. The initially prepared Na^-* state absorbs strongly at 560, 590 and 625 nm and weakly at 670 and 800 nm (see Fig. 1 and Table I) and takes ~700 fs to decay by undergoing CTTS. The CTTS electron transfer produces the contact pair containing Na^0, leading to some of the apparent decay of the visible transient bleach signals as well as the delayed rise of the 1150-nm Na^0 absorption on the same ~700-fs time scale. Geminate recombination on the ~1.5-ps time scale then causes a decay of the Na^0 absorption at 1150 nm. At the visible probe wavelengths, the cross-section of the Na^- produced by recombination is larger than that of the Na^0 lost due to recombination (Fig. 1), producing a further decay of the visible bleach signals. The simplicity of the delayed ejection model suggests that we have a good understanding of the rudiments of the CTTS process and that some of the more complex schemes invoked to explain CTTS dynamics following multiphoton excitation[10] are unnecessary.

The data in Figs. 3(a)–3(c) represent the first observation of the excited CTTS state and thus provide the first direct measure of the dynamics of charge transfer following one-photon excitation directly into a CTTS band. The fact that the excited state absorption is narrow and has a large oscillator strength implies that it arises from a bound–bound and not a bound–continuum transition. Thus, if the 590-nm absorption arises directly from the CTTS excited state(s), these states must lie at least 2.1 eV (590 nm) below the continuum in THF. Since the CTTS band of Na^- peaks near 1.7 eV (720 nm), this would imply that the ground state of sodide lies at least 3.8 eV below the continuum. The thermodynamics of sodide and solvated electrons in THF are not well known, so it is difficult to determine whether the assignment of such a stable Na^- species (and of CTTS excited states so far below the continuum) is reasonable. An alternate possibility is that the 590-nm excited state absorption arises from the neutral sodium core following excitation of one of the Na^- 3*s* electrons into the CTTS excited state. The idea is that the excited electron interacts only weakly with the sodium atom core, but serves to ''hold back'' the surrounding solvent so that the core has an absorption spectrum similar to that in the gas phase. When the excited electron is ejected by CTTS, THF molecules rush in to solvate the core, rapidly producing the equilibrium Na^0 spectrum measured by pulsed radiolysis (Fig. 1).[20] Whatever the origin of the 590-nm absorption, it is clearly correlated with the presence of the CTTS excited state. The importance of being able to monitor the dynamics of the CTTS excited state spectroscopically was pointed out in the introduction. Without a spectroscopic handle on the initially prepared CTTS state, the time scale for charge transfer can be inferred only indirectly from the appearance of the solvated electron because the appearance of the electron's absorption can be complicated by both solvation dynamics and internal relaxation.

The constraints imposed in fitting the delayed ejection model to the data also provide information about the identity of the Na^0 species. The shapes of the transients that can be fit by the model are quite sensitive to the choice of cross-sections assumed for the sodium atom product. Changing the shape of the Na^0 absorption in the model leads to generally poorer agreement with the data in Figs. 3 and 4. Thus, the success of the model indicates that the neutral sodium atom produced following CTTS is the same species that has been studied in the radiolysis of Na^+/THF solutions.[20,35] The radiation chemistry literature has always referred to this species as a (Na^+; e^-) moiety since it was unclear whether this entity is better identified as a sodium cation/solvated electron contact ion pair or as a neutral sodium atom. In our experiments, once the CTTS electron is removed from Na^-, breakdown of the Na^0 in the $Na^0 \bullet e^-$ pair to generate a $Na^+ : e^-$ contact ion pair would require the additional ejection and subsequent solvation of a second electron from the sodium atom core, as has been observed for the Cl atom following multiphoton excitation of the CTTS band of aqueous Cl^-.[11] It is also possible that the initial excitation might eject both valence electrons from sodide, an idea that would be consistent with early reports suggesting that the oscillator strength of the sodide CTTS transition is ~2.[36] If this were the case, then a better description of the CTTS process would be simultaneous ejection of two electrons: one that stays associated with the sodium cation core [forming a (Na^+; e^-) species] and a second that forms a contact pair with the (Na^+; e^-) species and eventually recombines to reform Na^- or dissociates to form a solvated electron. Unfortunately, our data do not allow us to distinguish whether one or two electrons are ejected upon photoexcitation of the CTTS transition, although further experiments are in progress. The fact that the equilibrium Na^0 absorption appears immediately following CTTS and shows no subsequent spectral dynamics, however, suggests to us that only one electron is ejected and that the species whose absorption spectrum is shown in Fig. 1 is better described as a neutral sodium atom.

The slight disagreement between the fits and the data in Figs. 3 and 4 suggests that solvation dynamics, which are not included in the delayed ejection model, do play a role in the CTTS process. One possible way in which solvation dynam-

ics could affect the observed pump–probe transients is via spectral diffusion of the ''hole'' created in the ground state bleach. Spectral diffusion results from the fact that the initial pulse excites only a subset of Na^- transitions that are in ''selected'' solvent configurations. This would leave a hole at the position of the excitation pulse in the ground state spectrum. The hole spreads after solvent fluctuations randomize the local environments, leading eventually to uniform bleaching of the absorption band. Our expectation, however, is that spectral hole-burning is not important in the transient spectroscopy shown in Figs. 3 and 4. Based on an analogy with the electronically similar hydrated electron, excitation of one of the $(s\rightarrow p)$-like transitions comprising the CTTS band should result in photobleaching an electronic progression of all three bands: Depletion of ground state Na^- species leads to ''replica holes'' at the positions of all three transitions originating from the ground state.[37] Thus, excitation anywhere within the band is expected to lead to nearly uniform bleaching with solvation dynamics playing little role in the transient bleach dynamics[16] except perhaps near the edges of the CTTS band.[37] We note that since the transition dipoles of the $3s\rightarrow p$ sub-bands are mutually orthogonal, it should be possible to observe the asymmetric solvent fluctuations that split the transitions by taking advantage of polarized transient hole-burning spectroscopy.[37,38] Our preliminary results using polarized pump and probe pulses, however, show little anisotropy, suggesting that bleaching dynamics are not important in the spectroscopy of the CTTS transition.

Since bleaching dynamics are not likely to be important in the spectroscopy of Na^-, the discrepancies between the delayed ejection model and the data in Figs. 3 and 4 likely result from solvation dynamics of the Na^0 species. The idea is that the neutral sodium product of the CTTS reaction is formed out of equilibrium with the surrounding solvent. The resulting solvent relaxation leads to spectral evolution of the Na^0 absorption, as discussed earlier in connection with the ''solvation'' model. The failure of the solvation model to fit the data makes it clear that solvation dynamics of the neutral sodium atom are not responsible for the bulk of the observed transient spectral changes. But the fact that the largest disagreement between the data and the delayed ejection model occurs for the 670-nm and 800-nm transients, however, suggests that solvation of Na^0 does play a secondary role in the observed spectroscopy. For example, solvation dynamics could be responsible for a slight delay in the appearance of the Na^0 absorption at 670 and 800 nm. The growth of an absorption at these two wavelengths would appear in the pump–probe experiments as a decay of the ground state bleach that is more rapid than that accounted for in the model, exactly what is observed in Figs. 3(d) and 3(e). It is also possible that solvation dynamics could shift the spectrum of the Na^-* excited state, causing it to pick up oscillator strength at the redder wavelengths, providing an alternate explanation for the more-rapid-than-expected decay of the bleach at these wavelengths. This idea is also consistent with the possibility that the 590-nm absorption results from the gas-phaselike core of Na^-*, whose absorption spectrum then undergoes a rapid shift upon solvation following ejection of the CTTS electron. We will continue to explore the solvation dynamics of Na^-* and Na^0 in future experiments; in the interim, however, it is reasonable to conclude that solvation plays an important but secondary role in the transient spectroscopy of the Na^- CTTS transition.

The geminate recombination dynamics of the ejected electron shown in Fig. 2 also provide insight into the mechanism underlying the CTTS transition of sodide in THF. Like what is observed in the photoionization of neat solvents,[28] increasing the excitation energy dramatically decreases the fraction of electrons that undergo geminate recombination. Our working hypothesis to explain this behavior is that the CTTS process spawns electrons that either can localize immediately adjacent to the neutral parent atom [''contact pair,'' as suggested by Eq. (2) and discussed in Ref. 8] or become trapped some distance away, as discussed further below. If the solvated electron is produced far from the Na^0 core, the disruption of the local solvent structure needed to regenerate the parent ion leads to a large free energy barrier to recombination. This free energy barrier makes it unlikely that recombination would occur even on diffusive time scales, similar to the recent observations of Kohler and coworkers.[39] The fact that very little decay is observed on the hundreds of ps time scale for either the solvated electron or the Na^0 species is consistent with this viewpoint. For those electrons that are ejected near the sodium atom core, minimal rearrangement of the local environment is required, significantly reducing the free energy barrier to recombination. Thus, we expect for this case that the solvation dynamics in THF that are known to occur on the $\sim$1.5-ps time scale[33] are effective for promoting recombination of electrons in the contact pair, consistent with the data in Figs. 2–4. It is interesting to note that this picture of geminate recombination as resulting from a contact pair is also consistent with the dynamics following CTTS excitation of aqueous iodide.[13]

Our hypothesis explaining the variation in the recombination fraction with excitation wavelength requires the existence of different pathways for electron ejection in the CTTS process. Based on the structure of the solvated electron in THF, we believe it is likely that there are two distinct mechanisms for electron production following CTTS. In water or alcohols, the solvated electron is confined within a localized solvent cavity, leading to an electronic absorption spectrum in the visible or near-IR. Solvated electrons in nonpolar fluids like THF, in contrast, have an absorption spectrum in the mid-IR, suggestive of a weakly localized object whose volume could encompass multiple solvent molecules.[40] Thus, the CTTS process of Na^- in THF involves expansion of the relatively compact CTTS excited state wave function into the more spatially extended ground state of the solvated electron. Excitation into the lowest energy CTTS band likely produces a solvated electron whose charge density remains centered near the sodium atom core upon expansion. The large spatial extent of the solvated electron's wave function virtually guarantees there will be some overlap with the neutral sodium core, allowing solvation dynamics to efficiently promote recombination of the contact pair [large k_2 in Eq. (3)]. The higher-lying CTTS excited states, on the other hand, are

expected to have highly distorted electronic wave functions that sample regions of the fluid farther from the sodium nucleus. Excitation of the higher-lying CTTS bands can thus result in a branching between rapid electron ejection to locations far into the solvent [large k_3 in Eq. (4)] and nonadiabatic relaxation into the lowest-lying CTTS excited state, which leads to more localized ejection and a higher probability for recombination. Following high-energy excitation, the time needed to localize electrons far into the solvent leads to an additional delay in the appearance of the electron's absorption.[29] The data presented in Fig. 2 are consistent with all of these ideas.

Finally, the data presented above offer some preliminary insight into the specific solvent motions underlying the CTTS phenomenon. The observed ~700-fs time for charge transfer does not match either of the previously measured times for dielectric solvation in THF.[33] One possibility is that the solvent motions needed to promote charge transfer are those driven by changes in size of the reacting species during CTTS: In addition to the expansion of the electron, the neutral sodium atom should be quite a bit smaller than the sodide anion. Computer simulations have shown that the translational solvent motions that accommodate solute size changes are quite a bit slower than the rotational motions associated with dielectric relaxation.[41] Thus, the rate-limiting step in the CTTS process may be the time needed for solvent molecule translation to allow the charge transfer to produce the stabilized sodium atom and solvated electron products. Another possibility is that the change in symmetry of the electronic wave function is responsible for the relatively slow ~700-fs CTTS electron transfer rate. For the case of aqueous halides, rapid solvent motions are easily able to induce adiabatic detachment of the *s*-like CTTS excited state into the *s*-like hydrated electron ground state.[7,8] For Na^-, however, production of the nodeless solvated electron ground state requires a nonadiabatic transition that destroys the node of the *p*-like CTTS excited-state wave function. Internal motions of the THF solvent molecules are unlikely to provide this nonadiabatic coupling, suggesting that specific, slower intermolecular motions are what drives the electron transfer. We are presently constructing nonadiabatic quantum molecular dynamics simulations, which in combination with additional pump–probe experiments, should help to identify the particular solvent motions involved and provide a clearer picture of all the details underlying the charge transfer process.

ACKNOWLEDGMENTS

This work was supported by a National Science Foundation CAREER award under Grant No. CHE-9733218. Benjamin J. Schwartz is a Cottrell Scholar of Research Corporation and an Alfred P. Sloan Foundation Research Fellow. We thank Sonia Connolly of Sundown Arts for development of the computer-A/D interface software used to collect the data, and the Foote research group at UCLA for assistance with the microsecond flash photolysis experiments. We also thank John Miller for providing the pulse radiolysis data for the Na^0/THF spectrum presented in Fig. 1 (Ref. 20), and Steve Bradforth for many stimulating discussions related to this work. Finally, we express our gratitude to the referee both for suggesting the use of the $Na^0 \cdot e^-$ contact pair as a way to include geminate recombination in the kinetic model without having to sacrifice the convenience of an analytical solution, and for making us aware of Ref. 36.

[1] For some recent review articles, see M. Maroncelli, J. Mol. Liq. **57**, 1 (1993); M. Cho and G. R. Fleming, Annu. Rev. Phys. Chem. **47**, 109 (1996); P. J. Rossky and J. D. Simon, Nature (London) **370**, 263 (1994); W. P. DeBoeij, M. S. Pshenichnikov, and D. A. Wiersma, Annu. Rev. Phys. Chem. **49**, 99 (1998).

[2] See, e.g., J. T. Hynes, in *Ultrafast Dynamics of Chemical Systems,* edited by J. D. Simon (Kluwer Academic, Netherlands, 1994), Ch. 13, p. 345; P. F. Barbara, T. J. Meyer, and M. A. J. Ratner, J. Phys. Chem. **100**, 13148 (1996).

[3] For an excellent review, see M. J. Blandamer and M. F. Fox, Chem. Rev. **70**, 59 (1970).

[4] See, e.g., J. Jortner, M. Ottolenghi, and G. Stein, J. Phys. Chem. **68**, 247 (1964); L. I. Grossweiner and M. S. Matheson, *ibid.* **61**, 1089 (1957); M. S. Matheson, W. A. Mulac, and J. Rabani, *ibid.* **67**, 261 (1963).

[5] D. Sexner, C. E. H. Dessent, and M. A. Johnson, J. Chem. Phys. **105**, 7231 (1996); L. Lehr, M. T. Zanni, C. Frischkorn, R. Weinkauf, and D. M. Neumark, Science **284**, 635 (1999).

[6] J. E. Combariza, N. R. Kestner, and J. Jortner, J. Chem. Phys. **100**, 2851 (1994).

[7] W.-S. Sheu and P. J. Rossky, Chem. Phys. Lett. **202**, 186 (1993); *ibid.* **213**, 233 (1993); J. Am. Chem. Soc. **115**, 7729 (1993); J. Phys. Chem. **100**, 1295 (1996).

[8] A. Staib and D. Borgis, J. Chem. Phys. **103**, 2642 (1995); D. Borgis and A. Staib, Chem. Phys. Lett. **230**, 405 (1994); A. Staib and D. Borgis, J. Chem. Phys. **104**, 9027 (1996); D. Borgis and A. Staib, J. Phys.: Condens. Matter **8**, 9389 (1996).

[9] F. H. Long, X. Shi, H. Lu, and K. B. Eisenthal, J. Phys. Chem. **98**, 7252 (1994); F. H. Long, H. Lu, X. Shi, and K. B. Eisenthal, Chem. Phys. Lett. **169**, 165 (1990); F. H. Long, H. Lu, and K. B. Eisenthal, J. Chem. Phys. **91**, 4413 (1989).

[10] H. Gelabert and Y. Gauduel, J. Phys. Chem. **100**, 13993 (1996); Y. Gauduel, H. Gelabart, and M. Ashokkumar, Chem. Phys. **197**, 167 (1995); Y. Gauduel, S. Pommeret, A. Migus, N. Yamada, and A. Antonetti, J. Opt. Soc. Am. B **7**, 1528 (1990).

[11] M. Assel, R. Laenen, and A. Laubereau, Chem. Phys. Lett. **289**, 267 (1998).

[12] J. A. Kloepfer, V. H. Vilchiz, V. A. Lenchenkov, and S. E. Bradforth, Chem. Phys. Lett. **298**, 120 (1998).

[13] J. Kloepfer, V. H. Vilchiz, V. Lenchenkov, and S. E. Bradforth, J. Chem. Phys. (submitted).

[14] For general reviews, see J. L. Dye, J. Phys. IV **1**, 259 (1992); J. L. Dye, Prog. Inorg. Chem. **32**, 327 (1984); J. Chem. Educ. **54**, 332 (1977).

[15] S. Matalon, S. Golden, and M. Ottolenghi, J. Phys. Chem. **73**, 3098 (1969); M. T. Lok, F. J. Tehan, and J. L. Dye, *ibid.* **76**, 2975 (1972).

[16] D. Huppert, P. M. Rentzepis, and W. S. Struve, J. Phys. Chem. **79**, 2850 (1975); D. Huppert and K. H. Bar-Eli, *ibid.* **74**, 3285 (1970); D. Huppert and P. M. Rentzepis, *ibid.* **64**, 191 (1976).

[17] W. A. Seddon and J. W. Fletcher, J. Phys. Chem. **84**, 1104 (1980).

[18] A. S. Ellaboudy, D. M. Holton, N. C. Pyper, P. P. Edwards, B. Wood, and W. McFarlane, Nature (London) **321**, 684 (1986); D. M. Holton, A. S. Ellaboudy, R. N. Edmonds, and P. P. Edwards, Proc. R. Soc. London, Ser. A **415**, 121 (1988).

[19] L. M. Dorfman, F. Y. Jou, and R. Wageman, Ber. Bunsenges. Phys. Chem. **75**, 681 (1971); F. Y. Jou and G. R. Freeman, Can. J. Phys. **54**, 3693 (1976).

[20] P. Piotr and J. R. Miller, J. Am. Chem. Soc. **113**, 5086 (1991); B. Bockrath and L. M. Dorfman, J. Phys. Chem. **79**, 1509 (1975); **77**, 1002 (1973).

[21] J. Schnitker, K. Motakabbir, P. J. Rossky, and R. A. Friesner, Phys. Rev. Lett. **60**, 456 (1988); P. J. Rossky and J. Schnitker, J. Phys. Chem. **92**, 4277 (1988).

[22] I. Hurley, T. R. Tuttle, and S. Golden, J. Chem. Phys. **48**, 2818 (1968).

[23] J. L. Dye, J. Phys. Chem. **84**, 1084 (1980).

[24] The advantage of using this configuration is that any instabilities which cause the OPA signal and idler pulse energies to drop also result in an increase in the residual energy of the 800-nm fundamental. Since the sum frequency process is bilinear in the energy of each input beam, the effects

of the fluctuations tend to cancel resulting in an exceptionally stable output.
[25] N. A. Anderson, Ph. D. thesis, University of Michigan (2000).
[26] T.-Q. Nguyen, I. Martini, J. Liu, and B. J. Schwartz, J. Phys. Chem. **104**, 237 (2000).
[27] Our choice of the ~500-nm excitation wavelength also helps to ensure that the build-up of photolysis products has little effect on the data because none of the long-lived species produced following excitation absorb at this wavelength.
[28] R. A. Crowell and D. M. Bartels, J. Phys. Chem. **100**, 17940 (1996); M. U. Sander, K. Luther, and J. Troe, Ber. Bunsenges. Phys. Chem. **97**, 953 (1993); J. L. McGowen, H. M. Ajo, J. Z. Zhang, and B. J. Schwartz, Chem. Phys. Lett. **231**, 504 (1994).
[29] The slower rise for 400-nm excitation is also consistent with the idea that detachment takes place only from the lowest CTTS state and that higher energy excitation requires a time-delay for non-adiabatic relaxation into the lowest state, as suggested by Sheu and Rossky in Ref. 7.
[30] Alternatively, the initially produced species could be thought of as a $Na^0 \bullet e^-$ contact pair, which would be spectroscopically indistinguishable from solvent-separated Na^0 and e^-, as discussed further below.
[31] As shown in Ref. 19, the absorption spectrum of the solvated electron in THF has a ''tail'' that extends well into the near-IR and visible. The molar extinction coefficient of the electron, however, is quite a bit smaller than that of Na^- or Na^0 at the visible probe wavelengths chosen for this study. At 1150 nm, however, the electron's absorption cross-section is nearly half that of Na^0. Since the cross-section for the electron at each wavelength is known, a term for the electron absorption can be added to the ''delayed ejection'' model without the introduction of any additional adjustable parameters. When such a term is added to the model, the fits are not significantly improved and the adjustable parameters (k_1, k_2, f and the Na^-* cross-sections) are unchanged within the error of the fit.
[32] Without introducing the contact atom:electron pair, the resulting kinetic scheme incorporating bimolecular recombination would involve Ricatti-type differential equations that have no analytic solution; see the papers in Ref. 28 for a discussion of more complex recombination schemes. It is worth reiterating that the physical presence of the contact pair cannot be detected spectroscopically: we assign the absorption spectrum of the contact pair as the sum of the individual Na^0 and $e^-_{solvated}$ absorptions.
[33] L. Reynolds, J. A. Gardecki, S. J. V. Frankland, M. L. Horng, and M. Maroncelli, J. Phys. Chem. **100**, 10337 (1996).
[34] Several studies have indicated that the dynamics of the solvent response depend on the details of the change in charge distribution upon excitation; see, e.g., B. M. Ladanyi and M. Maroncelli, J. Chem. Phys. **109**, 3204 (1998) or B. M. Ladanyi and R. M. Stratt, J. Phys. Chem. **100**, 1266 (1996). This means that the solvation dynamics of the monopolar change in charge associated with the CTTS excitation of sodide could be quite different from those measured for the dipolar excitation of the coumarin dye studied in Ref. 33.
[35] In Ref. 17, Seddon and Fletcher observe a transient absorption from Na^-/THF solutions in microsecond flash photolysis that looks very much like the Na^0 spectrum shown in Fig. 1. Seddon and Fletcher, however, assign this absorption to K^- produced by diffusive recombination following photoexcitation of Na^-. The data in Figs. 3 and 4 show the absorbing species is formed on a sub-picosecond time scale, consistent with assignment to Na^0. Thus, we believe that Seddon and Fletcher's assignment of the near-IR microsecond transient absorption to production of K^-, which has a very similar absorption spectrum to Na^0, is mistaken.
[36] M. G. DeBacker and J. L. Dye, J. Phys. Chem. **75**, 3092 (1971).
[37] B. J. Schwartz and P. J. Rossky, Phys. Rev. Lett. **72**, 3282 (1994); B. J. Schwartz and P. J. Rossky, J. Chem. Phys. **101**, 6917 (1994); K. A. Motakabbir, J. Schnitker, and P. J. Rossky, *ibid.* **90**, 6916 (1989).
[38] J. Yu and M. Berg, J. Phys. Chem. **97**, 1758 (1993); P. J. Reid, C. Silva, P. K. Walhout, and P. F. Barbara, Chem. Phys. Lett. **228**, 658 (1994).
[39] J. Peon, G. C. Hess, J.-M. L. Pecourt, T. Yuzawa, and B. Kohler, J. Phys. Chem. A **103**, 2460 (1999).
[40] H. T. Davis and R. G. Brown, Adv. Chem. Phys. **31**, 329 (1975). For a theoretical calculation of the solvated electron's structure in typical nonpolar liquids, see, e.g., Z. Liu and B. Berne, J. Chem. Phys. **99**, 9054 (1993).
[41] V. Tran and B. J. Schwartz, J. Phys. Chem. B **103**, 5570 (1999); D. Aherne, V. Tran, and B. J. Schwartz, J. Phys. Chem. (in press).